

Eigenfrequencies of two mutually interacting gas bubbles in an acoustic field

Masato Ida

Satellite Venture Business Laboratory, Gunma University, 1-5-1 Tenjin-cho, Kiryu-shi, Gunma 376-8515, Japan

E-mail : ida@vbl.gunma-u.ac.jp

(November 19, 2018)

Eigenfrequencies of two mutually interacting gas bubbles in an acoustic field are discussed theoretically and numerically. It is shown by a linear theory that a bubble interacting with a neighboring bubble has three eigenfrequencies that change with the distance between two bubbles, and the sign and magnitude of the primary Bjerknes force acting on bubbles also change according to the change in the eigenfrequencies.

PACS numbers: 43.20.+g, 47.55.Bx, 47.55.Dz, 47.55.Kf

INTRODUCTION

It is known that many bubbles levitated in a liquid form a stable structure named “bubble grapes” when a weak standing sound wave is applied [1–4]. In this stable structure, bubbles or clusters of them maintain a distance each other and tend not to collide, contrary to predictions given by the classical theory by Bjerknes which allows either only attraction or repulsion. The distance between bubbles or clusters in the structure is comparable to their sizes. A similar phenomenon can be observed in a strong acoustic field [5] in which bubbles form a complex filamentary structure varying slowly, whose scale is much smaller than the wavelength of the acoustic field.

In order to understand these phenomena, one should know thoroughly how the mutual interaction of the bubbles influences their acoustic properties. In Ref. [2], Zabolotskaya showed theoretically that the effective resonance frequencies of two interacting bubbles rise or fall as bubbles approach each other and that the variation in the resonance frequencies may sometimes causes the change of the sign of the secondary Bjerknes force, which is an interaction force acting between pulsating bubbles, at a certain distance. In Ref. [3], Doinikov and Zavtrak introduced a similar result by taking the multiple scattering of sound between two bubbles into account. They explain the origin of the change in the sign of the force as follows: When two bubbles oscillate in phase, their surfaces move against each other resulting in a stiffening of the bubbles. This may increase the effective resonance frequencies (or eigenfrequencies) of both bubbles and may sometimes cause the change in the sign of the force from attractive to repulsive.

Influences of mutual interaction have also been studied in regard to sonoluminescence [6,7]. In Ref. [6], Mettin et al. examined numerically the sign and magnitude of the secondary Bjerknes force acting between two small air bubbles in a strong acoustic field. They determined that even when the distance between two bubbles is much larger than their equilibrium sizes the magnitude of the force becomes much larger than that predicted by a linear theory, and the sign of the force changes near the dynam-

ical Brake threshold or around the *nonlinear* resonance frequency. In Ref. [7], Doinikov showed that a neighboring bubble drastically varies the magnitude and sign of the primary Bjerknes force, which an incident sound wave exerts on a bubble, in a strong acoustic field.

In this paper, following Zabolotskaya’s approach, the influences of the mutual interaction on the effective resonance frequencies of bubbles are theoretically examined in detail. As was pointed out and was mentioned previously, the variations in eigenfrequencies strongly affect the primary and secondary Bjerknes forces. This means that full understanding of the eigenfrequencies surely must be of help in knowing how the forces are changed by mutual interaction. In Sec. II A, we show that the variation in the eigenfrequencies with respect to the distance between two bubbles is more complicated than those expected by Zabolotskaya [2] and Doinikov and Zavtrak [3,4]. In Sec. II B, additionally, we discuss theoretically the influence of the mutual interaction on the amplitude of the bubble pulsation. In Sec. III, we show some numerical results of the primary Bjerknes force, acting on two interacting bubbles, by using a nonlinear model in order to verify the linear theory for the eigenfrequencies. When the frequency of an external sound is equivalent to an eigenfrequency of a bubble, the force vanishes because of the phase difference of $\pi/2$ between the sound and the bubble pulsation. Namely, by observing the points where the force vanishes, one can know how the eigenfrequencies changed by the interaction.

In the present study, an external sound field of weak or moderate amplitude with a frequency comparable to the partial resonance frequencies of bubbles is assumed.

I. MATHEMATICAL FORMULATION

A gas bubble levitated in a liquid pulsates when a sound wave is applied. The sound pressure at the bubble position drives the pulsation. When other bubbles (named “bubble 2” \sim “bubble N ”, where N is the number of existing bubbles) exist near the bubble (bubble 1), the pulsation of bubble 1 is also driven by the sound

wave scattered by the other bubbles. Namely, the driving pressure acting on bubble 1, p_{d1} , is expressed as

$$p_{d1} = p_{\text{ex}} + \sum_{j=2}^N p_{s1j}, \quad (1)$$

where p_{ex} and p_{s1j} are the sound pressures of the external sound field and the scattered wave emitted by bubble j , respectively, at the position of bubble 1. The pressure of the external sound can be considered uniform when the wavelength of the standing wave is much larger than the radii of the bubbles and the distance between bubbles. By assuming that those bubbles keep being spherically symmetric and the surrounding liquid is incompressible, the scattered pressure can be estimated with [6]

$$p_{s1j} \approx \frac{\rho}{r_{1j}} \frac{d}{dt} (R_j^2 \dot{R}_j), \quad (2)$$

where ρ is the density of the liquid, r_{1j} is the distance between the centers of bubble 1 and bubble j , R_j is the radius of bubble j , and the dot denotes the time derivative.

When the compressibility of the material surrounding the bubbles is completely negligible, one can use the RPNP equation [8]:

$$R_1 \ddot{R}_1 + \frac{3}{2} \dot{R}_1^2 - \frac{1}{\rho} p_{w1} = -\frac{1}{\rho} p_{d1}, \quad (3)$$

with

$$p_{w1} = \left(P_0 + \frac{2\sigma}{R_{10}} \right) \left(\frac{R_{10}}{R_1} \right)^{3\kappa} - \frac{2\sigma}{R_1} - \frac{4\mu \dot{R}_1}{R_1} - P_0,$$

for modeling the radial pulsation of bubbles, where P_0 is the static pressure, σ is the surface tension at the bubble surface, μ is the viscosity in the liquid, κ is the polytropic exponent of the gas inside the bubbles, and R_{10} is the equilibrium radius of bubble 1. Substitution of Eqs. (1) and (2) into Eq. (3) yields

$$R_1 \ddot{R}_1 + \frac{3}{2} \dot{R}_1^2 - \frac{1}{\rho} p_{w1} = -\frac{1}{\rho} \left[p_{\text{ex}} + \sum_{j=2}^N \frac{\rho}{r_{1j}} \frac{d}{dt} (R_j^2 \dot{R}_j) \right].$$

When the number of bubbles is two, this equation is reduced to

$$R_1 \ddot{R}_1 + \frac{3}{2} \dot{R}_1^2 - \frac{1}{\rho} p_{w1} = -\frac{1}{\rho} \left[p_{\text{ex}} + \frac{\rho}{D} \frac{d}{dt} (R_2^2 \dot{R}_2) \right], \quad (4)$$

where $D = r_{12}$ ($= r_{21}$). Exchanging 1 and 2 in the subscripts yields the model equation for bubble 2:

$$R_2 \ddot{R}_2 + \frac{3}{2} \dot{R}_2^2 - \frac{1}{\rho} p_{w2} = -\frac{1}{\rho} \left[p_{\text{ex}} + \frac{\rho}{D} \frac{d}{dt} (R_1^2 \dot{R}_1) \right] \quad (5)$$

with

$$p_{w2} = \left(P_0 + \frac{2\sigma}{R_{20}} \right) \left(\frac{R_{20}}{R_2} \right)^{3\kappa} - \frac{2\sigma}{R_2} - \frac{4\mu \dot{R}_2}{R_2} - P_0.$$

In the following sections, we present theoretical and numerical discussions regarding the above systems of equations (4) and (5).

II. LINEAR ANALYSIS

In this section, some basic properties of Eqs. (4) and (5) are discussed by means of linear theory. By assuming that the bubble pulsation can be represented as $R_1 = R_{10} + e_1$, $R_2 = R_{20} + e_2$, and $|e_1| \ll R_{10}$, $|e_2| \ll R_{20}$, Eqs. (4) and (5) are reduced to the following linear formulae:

$$\ddot{e}_1 + \omega_{10}^2 e_1 + \delta_1 \dot{e}_1 = -\frac{p_{\text{ex}}}{\rho R_{10}} - \frac{R_{20}^2}{R_{10} D} \ddot{e}_2, \quad (6)$$

$$\ddot{e}_2 + \omega_{20}^2 e_2 + \delta_2 \dot{e}_2 = -\frac{p_{\text{ex}}}{\rho R_{20}} - \frac{R_{10}^2}{R_{20} D} \ddot{e}_1, \quad (7)$$

where

$$\omega_{10} = \sqrt{\frac{1}{\rho R_{10}^2} [3\kappa P_0 + (3\kappa - 1) \frac{2\sigma}{R_{10}}]}$$

and

$$\omega_{20} = \sqrt{\frac{1}{\rho R_{20}^2} [3\kappa P_0 + (3\kappa - 1) \frac{2\sigma}{R_{20}}]}$$

are the partial resonance (angular) frequencies of bubble 1 and bubble 2, respectively,

$$\delta_1 = \frac{4\mu}{\rho R_{10}^2} \quad \text{and} \quad \delta_2 = \frac{4\mu}{\rho R_{20}^2}.$$

In the case where $\sigma \approx 0$, the system of equations (6) and (7) corresponds to that derived by Zabolotskaya [2] on the basis of Lagrangian formalism.

A. Eigenfrequencies of the linear system of equations

Let us analyze in detail the eigenfrequencies of the linear coupled system, although a brief discussion is shown in Ref. [2]. When only one bubble exists in an acoustic field and the frequency of the external sound is equivalent to the resonance frequency of the bubble, the phase difference between the bubble pulsation and the external sound becomes $\pi/2$, as is well known. According to this analogy, we call the frequency of an external sound an eigenfrequency of the linear coupled system when the phase difference between p_{ex} and e_1 (or p_{ex} and e_2) becomes $\pi/2$. We assume that the external sound pressure at the bubble position is written in a form of $p_{\text{ex}} = -P_a \sin \omega t$. A harmonic steady-state solution of the linear coupled system is

$$e_1 = K_1 \sin(\omega t + \phi_1), \quad (8)$$

where

$$K_1 = \frac{P_a}{R_{10}\rho} \sqrt{A_1^2 + B_1^2}, \quad (9)$$

$$\phi_1 = \tan^{-1} \left(\frac{B_1}{A_1} \right),$$

with

$$A_1 = \frac{H_1 F + M_2 G}{F^2 + G^2}, \quad (10)$$

$$B_1 = \frac{M_2 F - H_1 G}{F^2 + G^2}, \quad (11)$$

$$\begin{aligned} F &= L_1 L_2 - \frac{R_{10} R_{20}}{D^2} \omega^4 - M_1 M_2, \\ G &= L_1 M_2 + L_2 M_1, \\ H_1 &= L_2 + \frac{R_{20}}{D} \omega^2, \\ L_1 &= (\omega_{10}^2 - \omega^2), \quad L_2 = (\omega_{20}^2 - \omega^2), \\ M_1 &= \delta_1 \omega, \quad M_2 = \delta_2 \omega. \end{aligned}$$

Here the solution for only bubble 1 is shown. The phase difference ϕ_1 becomes $\pi/2$ when

$$A_1 = 0. \quad (12)$$

It should be noted that a case in which both A_1 and B_1 become zero does not exist. From Eqs. (10) and (11), one obtains

$$A_1^2 + B_1^2 = \frac{H_1^2 + M_2^2}{F^2 + G^2} \left(\frac{P_a}{R_{10}\rho} \right)^2.$$

The numerator of this equation always has a nonzero value since $M_2 > 0$; this result denies the existence of the case where both $A_1 = 0$ and $B_1 = 0$ are true. It should be noted also that $F^2 + G^2$ appearing in the denominator of Eq. (10) always has a nonzero value. When $G = 0$, F is reduced to

$$F = -\frac{M_2}{M_1} L_1^2 - \frac{R_{10} R_{20}}{D^2} \omega^4 - M_1 M_2.$$

This has a nonzero, negative value because of $M_2 L_1^2 / M_1 \geq 0$, $R_{10} R_{20} \omega^4 / D^2 > 0$ and $M_1 M_2 > 0$. This result means that no case exists where both $F = 0$ and $G = 0$ are true. In a consequence, Eq. (12) is reduced to

$$H_1 F + M_2 G = 0. \quad (13)$$

In the following, we analyze this equation.

When the viscous terms in Eq. (13) are negligible (but exist), one can easily obtain the solutions of this equation. By assuming that $M_1 \approx 0$ and $M_2 \approx 0$, one obtains

$$H_1 F = 0,$$

or

$$F \approx L_1 L_2 - \frac{R_{10} R_{20}}{D^2} \omega^4 = 0 \quad (14)$$

and

$$H_1 = L_2 + \frac{R_{20}}{D} \omega^2 = 0. \quad (15)$$

Equation (14) corresponds to that given in Ref. [2], and is symmetric; namely, exchanging 1 and 2 (or 10 and 20) on the subscripts of variables in this equation yields the same equation. This means that two bubbles have the same eigenfrequencies.

The solutions of Eq. (14) are

$$\omega_{1\pm}^2 = \frac{\omega_{10}^2 + \omega_{20}^2 \pm \sqrt{(\omega_{10}^2 - \omega_{20}^2)^2 + 4\omega_{10}^2 \omega_{20}^2 \frac{R_{10} R_{20}}{D^2}}}{2(1 - R_{10} R_{20} / D^2)}. \quad (16)$$

Those solutions can be rewritten approximately as follows in the case where the distance D is large enough and $\omega_{10} > \omega_{20}$:

$$\omega_{1+}^2 \approx \left[1 + \left(\frac{\omega_{10}^2}{\omega_{10}^2 - \omega_{20}^2} \right) \left(\frac{R_{10} R_{20}}{D^2 - R_{10} R_{20}} \right) \right] \omega_{10}^2 \quad (17)$$

and

$$\omega_{1-}^2 \approx \left[1 - \left(\frac{\omega_{20}^2}{\omega_{10}^2 - \omega_{20}^2} \right) \left(\frac{R_{10} R_{20}}{D^2 - R_{10} R_{20}} \right) \right] \omega_{20}^2. \quad (18)$$

For $D \sim \infty$, the former and the latter one converge to ω_{10}^2 and ω_{20}^2 , respectively. As the bubbles approach each other, the former increases and the latter decreases; namely, the higher eigenfrequency becomes higher and the lower one becomes lower.

In the case of $\omega_{10} < \omega_{20}$ and large D , the solutions (16) are reduced to

$$\omega_{1+}^2 \approx \left[1 + \left(\frac{\omega_{20}^2}{\omega_{20}^2 - \omega_{10}^2} \right) \left(\frac{R_{10} R_{20}}{D^2 - R_{10} R_{20}} \right) \right] \omega_{20}^2 \quad (19)$$

and

$$\omega_{1-}^2 \approx \left[1 - \left(\frac{\omega_{10}^2}{\omega_{20}^2 - \omega_{10}^2} \right) \left(\frac{R_{10} R_{20}}{D^2 - R_{10} R_{20}} \right) \right] \omega_{10}^2. \quad (20)$$

Same as the result for $\omega_{10} > \omega_{20}$, the higher eigenfrequency becomes higher and the lower one becomes lower as D decreases.

The solution of Eq. (15) given for the first time is

$$\omega_1^2 = \frac{\omega_{20}^2}{1 - R_{20}/D}. \quad (21)$$

This converges to ω_{20}^2 for an infinite D and increases with decreasing D . In contrast with Eq. (14), Eq. (15) is asymmetric; namely this serves to break the symmetry of the Zabolotskaya's result mentioned above.

The present results show that, when the viscous effect of the surrounding liquid is negligible and the radii of the bubbles are not equivalent, the bubbles have three asymmetric eigenfrequencies; one is the “fundamental eigenfrequency” that converges to the partial resonance frequency of a corresponding bubble for an infinite D , and the remaining two are the “subeigenfrequencies” that converge to the resonance frequency of a neighboring bubble. One of the subeigenfrequencies always increases as bubbles approach each other. The other subeigenfrequency decreases (increases) and the fundamental eigenfrequency increases (decreases) when the partial resonance frequency of the bubble is higher (lower) than that of the neighboring bubble.

Now we discuss briefly the case of identical bubbles. When two bubbles have the same radii and pulsate in phase, Eq. (6) is reduced to

$$\left(1 + \frac{R_{10}}{D}\right) \ddot{e}_1 + \omega_{10}^2 e_1 + \delta_1 \dot{e}_1 = -\frac{p_{\text{ex}}}{\rho R_{10}}.$$

This equation has only one eigenfrequency [2] of

$$\omega_1^2 = \frac{\omega_{10}^2}{1 + R_{10}/D}, \quad (22)$$

which converges to ω_{10}^2 for infinite D and decreases with decreasing D . Using this example, we here carry out quantitative comparison between the model used here and previous ones. In Ref. [10], Kobelev and Ostrovskii discussed the eigenfrequency of two interacting bubbles by means of a mathematical model in which the surface tension and viscosity are neglected and the potential field forming between the bubbles is accurately described by the method of images. The model predicts only two eigenfrequencies when $R_{10} \neq R_{20}$, as in Zabolotskaya's model, and gives $\omega_1 = \sqrt{\ln 2} \omega_{10} \simeq 0.832 \omega_{10}$ when $R_{10} = R_{20}$ and both bubbles make contact with each other, i.e., $D = 2R_{10}$. In Ref. [11], Zavtrak also discussed the eigenfrequency of the present case by means of a mathematical model in which multiple scattering between two bubbles is taken into account by the Legendre polynomial expansion. In the case of $D = 2R_{10}$, Zavtrak's model gives $\omega_1 \simeq 0.832 \omega_{10}$, which is in close agreement with the result obtained by Kobelev and Ostrovskii. However, Eq. (22) gives $\omega_1 \simeq 0.816 \omega_{10}$ which is lower by about 2 % than these values. This quantitative discrepancy is caused from the difference of functions for describing the scattered sound wave by a bubble. The amplitude of the scattered wave is assumed to be inversely proportional to D in the model used here (See Eq. (2)), while those in the models in Refs. [10,11] are approximated by an expansion function. Namely, the amplitude of the scattered wave at the position of a neighboring bubble is estimated differently. The influence of

this difference becomes stronger as D decreases. However, all models predict the same result in a qualitative sense, which reveals the downward shift of the eigenfrequency.

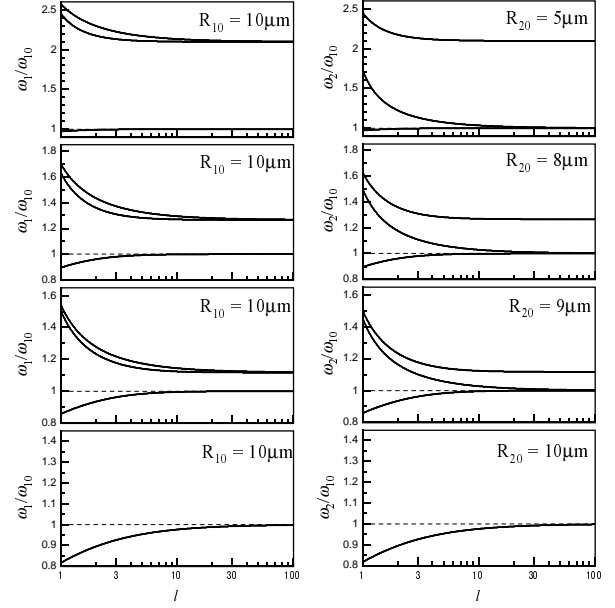


FIG. 1. The eigenfrequencies of bubbles 1 (ω_1) and 2 (ω_2) for $R_0 \sim 10 \mu\text{m}$ and $\mu \approx 0$ normalized by ω_{10} . The dashed line denotes the line of $\omega_j/\omega_{10} = 1$.

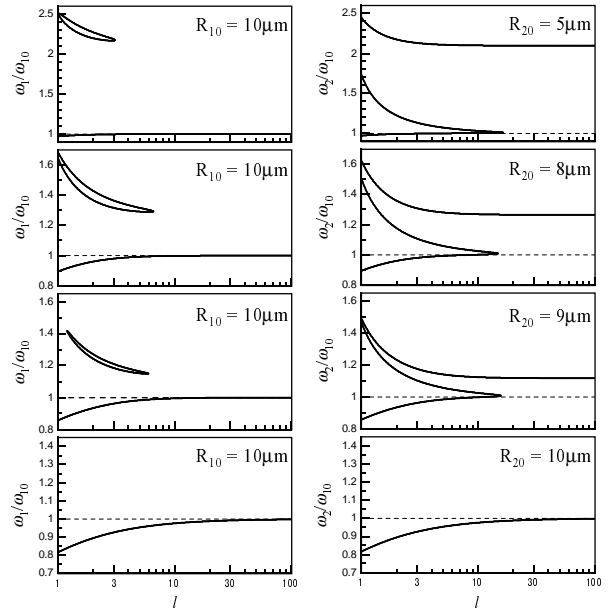


FIG. 2. The eigenfrequencies for $R_0 \sim 10 \mu\text{m}$ normalized by ω_{10} . The dashed line denotes the line of $\omega_j/\omega_{10} = 1$.

Figure 1 shows the eigenfrequencies as a function of $l = D/(R_{10} + R_{20})$, in the case where the viscous effect

is negligible. Here, the parameters are set to $\rho = 1000$ kg/m³, $P_0 = 1$ atm, $\sigma = 0.0728$ N/m, $\mu \approx 0$, and $\kappa = 1.4$. Equations (16) and (21) are used in plotting those graphs since Eqs. (17)–(20) provide a less-accurate result for small D . The radius of bubble 1 is fixed to $10\text{ }\mu\text{m}$ and that of bubble 2 varies from $5\text{ }\mu\text{m}$ to $15\text{ }\mu\text{m}$. The eigenfrequencies shown in those graphs are normalized with the partial resonance frequency of bubble 1, ω_{10} . As discussed above, three eigenfrequencies changing with the distance between bubbles appear in each graph except for the case of $R_{10} = R_{20}$ where only one decreasing eigenfrequency appears. It should be noted that the larger bubble, whose partial resonance frequency is lower than that of the smaller bubble, has the highest eigenfrequency among those of a pair of bubbles. This result is inconsistent with the opinion represented in Refs. [3,4] in which it is assumed that the effective resonance frequency of the smaller bubble rises faster than that of the larger bubble when two bubbles approach each other.

Now we present numerical solutions of Eq. (13) for examining the influences of viscosity on eigenfrequency. Figures 2–4 show the results obtained by using $\mu = 1.137 \times 10^{-3}$ kg/(m s) that corresponds to the viscosity of water at room temperature. From those figures, we can observe that, as the viscous effect grows strong, i.e., the mean radii of the two bubbles become smaller, the subeigenfrequencies vanish gradually from the large-distance region (and sometimes from the small-distance region) and only the fundamental eigenfrequency remains. In the case of $R_1 = 1\text{ }\mu\text{m}$, the subeigenfrequencies of a larger bubble disappear, and when the sizes of two bubbles are close each other the fundamental eigenfrequency and the higher one of subeigenfrequencies of a smaller bubble vanish in the small-distance region.

In the case of $R_1 = 0.1\text{ }\mu\text{m}$, it is difficult to distinguish the subeigenfrequencies from the fundamental one since only a smooth curve, which decreases monotonically with decreasing l , appears in the graphs. (The eigenfrequency of the smaller bubble remaining in the small-distance region may be the lower one of the subeigenfrequencies.) This result means that in a high-viscosity case the effective resonance frequencies of both bubbles decrease monotonically as l decreases.

These results show that the influence of the mutual interaction on the eigenfrequencies depends on the viscosity of the surrounding material and is weakened as the viscous effect becomes stronger, i.e., the threshold of the distance for the appearance of the subeigenfrequencies is shortened.

From the results shown in Fig. 2, we can expect that when $R_1 = 10\text{ }\mu\text{m}$, $R_2 = 8\text{ }\mu\text{m}$, and $\omega = 1.4\omega_{10}$, for example, the signs of the primary Bjerknes force acting on bubbles 1 and 2 change twice as the two bubbles approach each other since the curves shown in the figure for this case close with the line $\omega_j/\omega_{10} = 1.4$ ($j = 1, 2$) at two points. We can expect also from the results shown in Fig. 3 that when $R_1 = 1\text{ }\mu\text{m}$, $R_2 = 0.8\text{ }\mu\text{m}$, and $\omega = 1.1\omega_{10}$, the sign of the force acting on bubble 1

changes once during the approach since the curves for this case close with the line $\omega_1/\omega_{10} = 1.1$ at one point. Such an influence of the mutual interaction on the primary Bjerknes force is discussed in Sec. III.

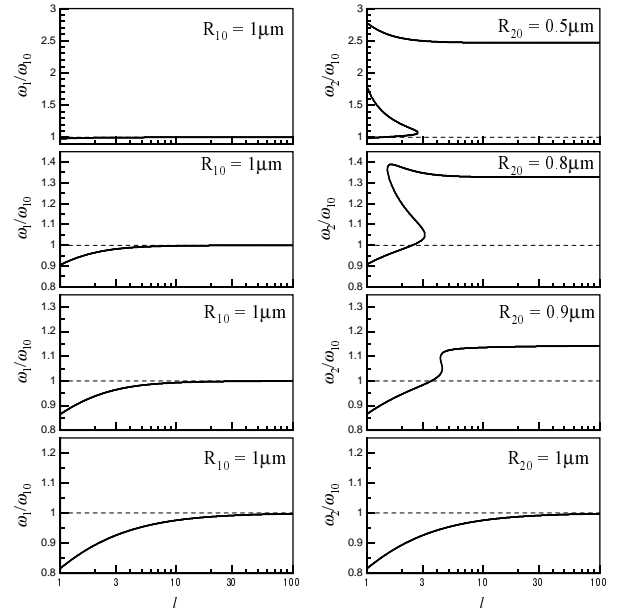


FIG. 3. The eigenfrequencies for $R_0 \sim 1\text{ }\mu\text{m}$ normalized by ω_{10} . The dashed line denotes the line of $\omega_j/\omega_{10} = 1$.

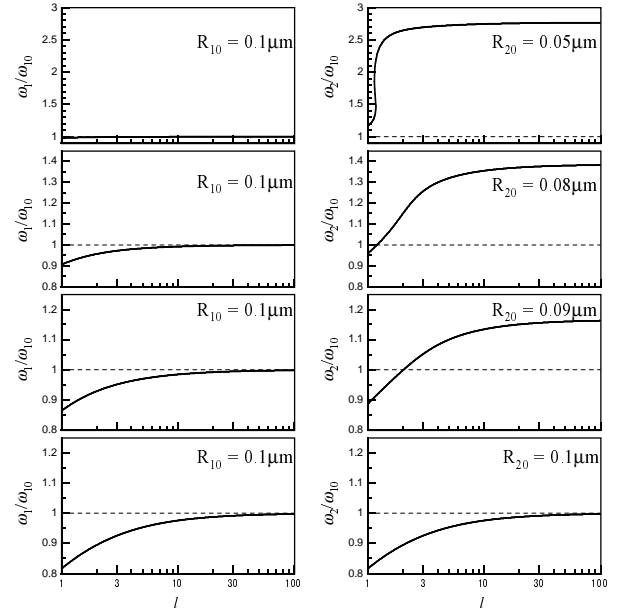


FIG. 4. The eigenfrequencies for $R_0 \sim 0.1\text{ }\mu\text{m}$ normalized by ω_{10} . The dashed line denotes the line of $\omega_j/\omega_{10} = 1$.

B. Amplitude of linear pulsation of two coupled bubbles

Next, we briefly discuss the amplitude of the bubble pulsation. By substituting Eqs. (10) and (11) into Eq. (9) and rearranging it, one obtains

$$K_1^2 = \frac{H_1^2 + M_2^2}{F^2 + G^2} \left(\frac{P_a}{R_{10}\rho} \right)^2. \quad (23)$$

When ω is far apart from the partial resonance frequencies of both bubbles and the viscous term is negligible, Eq. (23) is reduced to

$$K_1^2 \approx \left(\frac{L_2 + R_{20}\omega^2/D}{L_1 L_2 - R_{10}R_{20}\omega^4/D^2} \right)^2 \left(\frac{P_a}{R_{10}\rho} \right)^2.$$

Furthermore, neglecting the second order term of R_{j0}/D reduces this to

$$K_1^2 \approx \left(\frac{L_2 + R_{20}\omega^2/D}{L_1 L_2} \right)^2 \left(\frac{P_a}{R_{10}\rho} \right)^2 \\ = \left[1 + \left(\frac{R_{20}\omega^2}{\omega_{20}^2 - \omega^2} \right) \frac{1}{D} \right]^2 \left(\frac{1}{L_1} \right)^2 \left(\frac{P_a}{R_{10}\rho} \right)^2. \quad (24)$$

As D decreases, the amplitude K_1 increases when $\omega_{20} > \omega$, and decreases when $\omega_{20} < \omega$. Physically, this result can be understood as follows: When ω_{20} is sufficiently larger than ω , the scattered wave due to bubble 2 oscillates in phase with the external sound. In this case, the amplitude of the driving pressure acting on bubble 1 increases (See Eq. (6)); thus, the pulsation amplitude of bubble 1 is increased. In contrast, when ω_{20} is sufficiently smaller than ω , the scattered wave due to bubble 2 oscillates out of phase with the external sound; this results in the decrease of the pulsation amplitude.

Now we consider the case where two bubbles have the same radii and the frequency of the external sound is equivalent to their partial resonance frequencies, i.e., $R_{10} = R_{20}$ and $\omega = \omega_{10} = \omega_{20}$. This setting reduces Eq. (23) to

$$K_1^2 = \frac{1}{(R_{10}^2\omega_{10}^2/D^2 + \delta_1^2)\omega_{10}^2} \left(\frac{P_a}{R_{10}\rho} \right)^2.$$

This equation shows that the amplitude of the bubble pulsation decreases with decreasing D . This result can be explained as follows: The decrease of the eigenfrequency represented in Eq. (22) causes the difference between the sound frequency and the effective resonance frequency; resultantly, the amplitude of pulsation decreases. Such a decrease in the pulsation amplitude of identical two small near-resonance bubbles ($R_0 = 1.5 \mu\text{m}$) in a viscous liquid is shown in Ref. [12] by employing a direct-numerical-simulation technique. The present theory may explain the numerical result.

III. NUMERICAL EXPERIMENT

In this section, we show numerical results obtained by using the full system of nonlinear equations [(4) and (5)] and sufficiently small amplitude of sound in order to verify the linear theory given in the last section. We investigate the variations in eigenfrequencies by observing the primary Bjerknes force which is a time-averaged force acting on a bubble when the external sound field has a spatial gradient. The primary Bjerknes force [13] is expressed as

$$\mathbf{F}_j = -\frac{4\pi}{3} \langle R_j^3 \nabla p_{\text{ex}} \rangle, \quad (25)$$

where $\langle \dots \rangle$ denotes the time average over a period of the external sound. As was mentioned previously, the phase difference between the external sound and the bubble pulsation becomes $\pi/2$ when the sound frequency is equivalent to the resonance frequency of a bubble. In this situation, furthermore, the primary Bjerknes force vanishes as the result of the inner product by Eq. (25). This means that we can observe the eigenfrequencies of interacting bubbles by examining the conditions under which the magnitude of the force becomes zero.

Here we assume that the external standing wave field is in a form of

$$p_{\text{ex}}(z, t) = -P_a(z) \sin(\omega t)$$

with $P_a(z) = P_s \sin(kz)$, where z is the spatial coordinate vertical to the pressure nodes, $P_a(z)$ is the amplitude of the standing wave field at z , and k is the wave number of the standing wave field. This assumption yields

$$\nabla p_{\text{ex}}(z, t) = k \frac{\cos(kz)}{\sin(kz)} p_{\text{ex}}(z, t) \mathbf{z}, \quad (26)$$

where \mathbf{z} is the unit vector in the z direction. Substitution of Eq. (26) into Eq. (25) results in

$$\mathbf{F}_j = -\frac{4\pi}{3} k \frac{\cos(kz_j)}{\sin(kz_j)} f_j \mathbf{z}$$

with

$$f_j = \langle R_j^3 p_{\text{ex}}(z_j, t) \rangle, \quad (27)$$

where z_j is the position of bubble j in the z coordinate. The method for computing the force is the same as what used in Refs. [6,7]. The full system of nonlinear equations of (4) and (5) is solved numerically by the 4th-order Runge-Kutta method, and f_j is then computed with R_j given by the numerical computation. The time average in Eq. (27) is done over a sufficiently large period after the transition has decayed. Here we assume that the wavelength of the external sound is much larger than the distance between the bubbles, and thus, $p_{\text{ex}}(z_1, t) = p_{\text{ex}}(z_2, t)$.

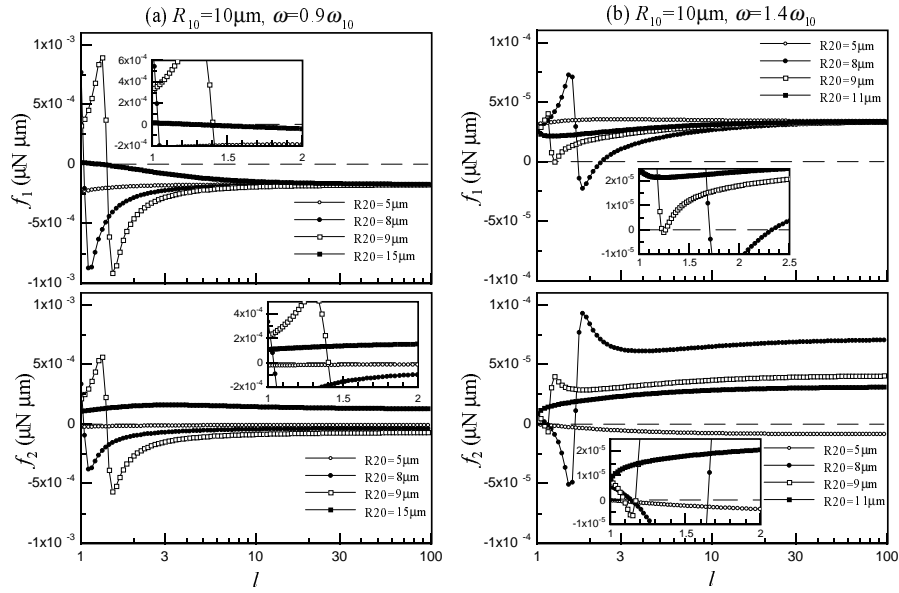


FIG. 5. $f_j - l$ curves for $R_{10} = 10 \mu\text{m}$ and different values of R_{20} . The sound frequency is set to $\omega = 0.9\omega_{10}$ (a) and $1.4\omega_{10}$ (b), and the sound amplitude is $0.001P_0$. The theoretical values of (l_1, l_2) , where l_1 and l_2 are the normalized distances at which $f_1 = 0$ and $f_2 = 0$, respectively, given by Eq. (13) are (a): (1.038, 1.038) for $R_{20} = 8 \mu\text{m}$, (1.402, 1.402) for $R_{20} = 9 \mu\text{m}$, (1.279, None) for $R_{20} = 15 \mu\text{m}$ and (b): (None, 1.362) for $R_{20} = 5 \mu\text{m}$, (1.703 and 2.330, 1.139 and 1.649) for $R_{20} = 8 \mu\text{m}$, (1.224 and 1.258, 1.089 and 1.166) for $R_{20} = 9 \mu\text{m}$.

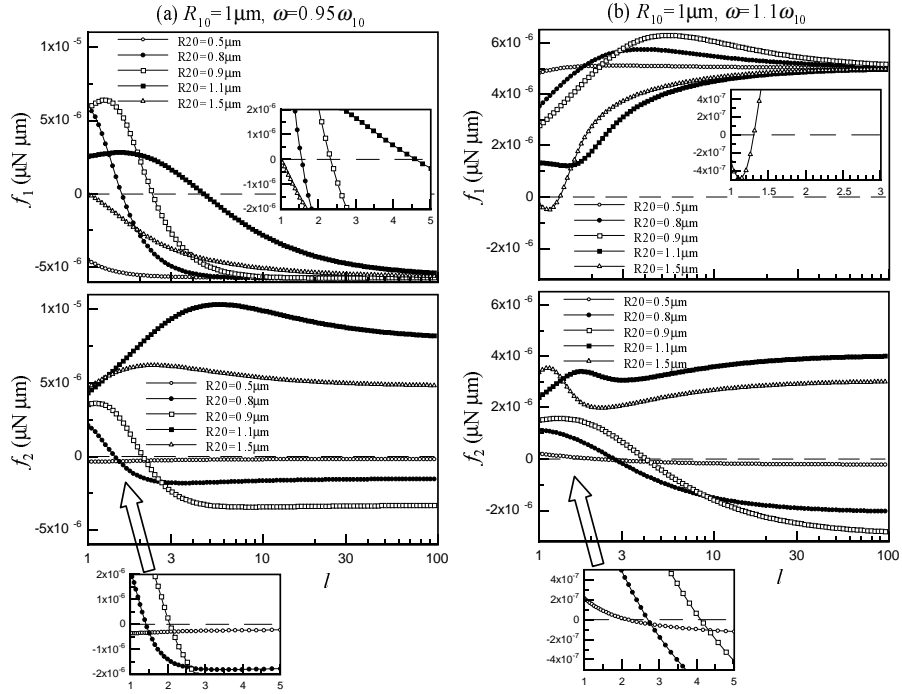


FIG. 6. $f_j - l$ curves for $R_{10} = 1 \mu\text{m}$ and different values of R_{20} . The sound frequency is set to $\omega = 0.95\omega_{10}$ (a) and $1.1\omega_{10}$ (b), and the sound amplitude is $0.01P_0$. The theoretical values of (l_1, l_2) given by Eq. (13) are (a): (1.574, 1.427) for $R_{20} = 0.8 \mu\text{m}$, (2.355, 2.077) for $R_{20} = 0.9 \mu\text{m}$, (4.761, None) for $R_{20} = 1.1 \mu\text{m}$, (1.049, None) for $R_{20} = 1.5 \mu\text{m}$ and (b): (None, 2.637) for $R_{20} = 0.5 \mu\text{m}$, (None, 2.789) for $R_{20} = 0.8 \mu\text{m}$, (None, 4.279) for $R_{20} = 0.9 \mu\text{m}$, (1.309, None) for $R_{20} = 1.5 \mu\text{m}$.

Figures 5–7 show $f_j - l$ curves for the cases of $R_{10} = 10 \mu\text{m}$, $R_{10} = 1 \mu\text{m}$ and $R_{10} = 0.1 \mu\text{m}$, respectively. Here the system of Eqs. (4) and (5) is used; namely, the compressibility of the surrounding material is neglected. The amplitude of the external sound at the bubble position is assumed as $P_a = 0.001P_0$, $0.01P_0$ and $0.1P_0$ for $R_{10} = 10 \mu\text{m}$, $1 \mu\text{m}$ and $0.1 \mu\text{m}$ cases, respectively. The frequency ω of the external sound is set to $0.9\omega_{10}$ and $1.4\omega_{10}$ for $R_{10} = 10 \mu\text{m}$, $0.95\omega_{10}$ and $1.1\omega_{10}$ for $R_{10} = 1 \mu\text{m}$, and $0.8\omega_{10}$ for $R_{10} = 0.1 \mu\text{m}$. In those graphs, we can observe some points where the primary Bjerknes force vanishes. The normalized distances at the points, given theoretically by solving Eq. (13) as a function of D with the given ω , are listed in the captions of those figures. These theoretical values are in good agreement with the numerical ones represented in those graphs. This result confirms our prediction that the sign of the primary Bjerknes force changes at distances where one of the eigenfrequencies becomes equivalent to the sound frequency.

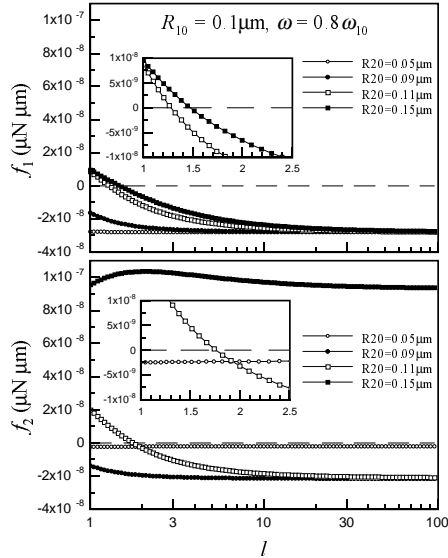


FIG. 7. $f_j - l$ curves for $R_{10} = 0.1 \mu\text{m}$ and different values of R_{20} . The sound frequency is $\omega = 0.8\omega_{10}$ and the sound amplitude is $0.1P_0$. The theoretical values of (l_1, l_2) given by Eq. (13) are $(1.279, 1.803)$ for $R_{20} = 0.11 \mu\text{m}$, $(1.474, \text{None})$ for $R_{20} = 0.15 \mu\text{m}$.

IV. CONCLUSION

In the present study, the dependency of the eigenfrequencies of two mutually interacting bubbles on the distance between the bubbles was theoretically determined concretely and in detail. The dependency is more intricate than those predicted or assumed previously by sev-

eral authors [2–4]. It was shown also that the eigenfrequencies depend also on the viscosity of the bubbles' surrounding material, unlike the partial natural frequency. Moreover, the present theory was verified numerically by observing the primary Bjerknes force acting on bubbles. These present results may be reasonable for understanding the reversal of sign of the secondary Bjerknes force [2–4,6] and the pattern formations of bubbles or clusters of them in an acoustic field [1,5]. As was pointed out in Sec. II A, Zabolotskaya's theory predicts that both bubbles interacting with each other have the same eigenfrequencies. This result may give rise to simultaneous phase changes of the bubbles, e.g., from in-phase to out-of-phase with the external sound, and, as a result, may deny the reversal of the sign. The asymmetric eigenfrequencies derived in the present paper may be able to describe the reversal of the sign more accurately. (This subject will be discussed in a future paper.) Furthermore, these present results will also affect understandings on some related subjects such as acoustic localization [14] and superresonances [15], which were investigated by employing a system containing only identical bubbles.

-
- [1] Y. A. Kobelev, L. A. Ostrovskii, and A. M. Sutin, JETP Lett. **30**, 395 (1979).
 - [2] E. A. Zabolotskaya, Sov. Phys. Acoust. **30**, 365 (1984).
 - [3] A. A. Doinikov and S. T. Zavtrak, Phys. Fluids **7**, 1923 (1995).
 - [4] A. A. Doinikov and S. T. Zavtrak, J. Acoust. Soc. Am. **99**, 3849 (1996).
 - [5] I. Akhatov, U. Parlitz, and W. Lauterborn, J. Acoust. Soc. Am. **96**, 3627 (1994); W. Lauterborn, T. Kurz, R. Mettin, and C. D. Ohl, Adv. Chem. Phys. **110**, 295 (1999).
 - [6] R. Mettin, I. Akhatov, U. Parlitz, C. D. Ohl, and W. Lauterborn, Phys. Rev. E **56**, 2924 (1997).
 - [7] A. A. Doinikov, Phys. Rev. E **62**, 7516 (2000).
 - [8] W. Lauterborn, J. Acoust. Soc. Am. **59**, 283 (1976).
 - [9] J. B. Keller and M. Miksis, J. Acoust. Soc. Am. **68**, 628 (1980).
 - [10] Yu. A. Kobelev and L. A. Ostrovskii, Sov. Phys. Acoust. **30**, 427 (1984).
 - [11] S. T. Zavtrak, Sov. Phys. Acoust. **33**, 145 (1987).
 - [12] M. Ida and Y. Yamakoshi, Jpn. J. Appl. Phys. **40**, 3846 (2001).
 - [13] A. I. Eller, J. Acoust. Soc. Am. **43**, 170 (1968); L. A. Crum and A. I. Eller, J. Acoust. Soc. Am. **48**, 181 (1969).
 - [14] Z. Ye and A. Alvarez, Phys. Rev. Lett. **80**, 3503 (1998).
 - [15] C. Feuillade, J. Acoust. Soc. Am. **98**, 1178 (1995).